CFD Simulations on an Up-Scaled Experiment and Determination of the Heat Transfer Coefficient for High Rayleigh-Number Natural Convection in Water

Zhi Yang
Gesellschaft für Anlagen- und Reaktorsicherheit (GRS) gGmbH
Boltzmannstraße 14, 85748 Garching
zhi.yang@grs.de

David Sonntag, Christoph Bratfisch, Marco K. Koch
Plant Simulation and Safety Group (PSS), Ruhr-Universität Bochum (RUB)
Universitätsstraße 150, 44801 Bochum
sonntag@pss.rub.de, bratfisch@pss.rub.de, koch@pss.rub.de
ORCID: 0000-0001-9524-9252, 0000-0003-4016-079X, 0000-0001-7260-5250

ABSTRACT

Innovative designs of LW-SMR foresee water filled pools as a heat sink, in which the SMR containment is partly or fully immersed. For safety assessment, the heat transferred from the containment to the water pool, e.g., in the case of a loss of coolant accident (LOCA), has to be correctly estimated. Current correlations only predict the heat transfer for Rayleigh-numbers $\leq 10^{12}$. In this work, the heat transfer is determined by analysing comparative CFD simulations using ANSYS CFX as well as OpenFOAM, regarding a selected experiment. The geometry of the experimental facility is scaled up to $15\,m$, to achieve Rayleigh-numbers of $> 10^{15}$, which is comparable to a generic submerged SMR concept.

INTRODUCTION

Specific light water cooled small modular reactor (LW-SMR) concepts, as for example the French NUWARD SMR, are designed as integral pressurised water reactors (iPWR). A vertical, cylindrical containment vessel (CV), including the reactor pressure vessel (RPV) and all primary circuit components, is fully submerged in deep water pools to passively cool the CV in case of a LOCA. In consequence of these postulated scenarios, the space between the RPV and the CV fills up with hot steam and water. As a result, the CV heats up, inducing an upward streaming free convection flow in the water pool, adjacent to the outer CV surface. Similar effects can occur in selected conventional nuclear power plants, since RPV cavity flooding is used as an in-vessel melt retention strategy [1; 2].

The dimensionless heat transfer coefficient (Nusselt-number (Nu)) for natural convection, is a function of the Rayleigh-number (Ra), the product of the Grashof- and Prandtl-number (Gr, Pr), is proportional to the third power of the characteristic length L represented by the height of the heated surface:

$$\mathrm{Nu} = \frac{\alpha\, L}{\lambda} = f(\mathrm{Ra}) \tag{1}$$

$$\mathrm{Ra} = \mathrm{Gr}\,\mathrm{Pr} = \frac{\vec{g}\,\beta\,\delta T\,L^3}{\nu^2}\mathrm{Pr} \tag{2}$$

Present correlations are limited to $\mathrm{Ra} \leq 10^{12}$ and thereby are restricted to low characteristic lengths for water pools. In (1) α describes the heat transfer coefficient. In (2) δT is a temperature difference of the heated surface and ambient fluid and $\vec{g}$ is the gravitational acceleration. The thermal conductivity λ and the kinematic viscosity ν are taken at average bulk fluid temperature. The thermal expansion coefficient β is considered to be constant along δT according to Boussinesq. In this work the experiment of Giel and Schmidt [3] from 1986 is modelled and used to validate CFD-simulations concerning boundary layers. In the experiment a maximum Rayleigh-number of $8 \cdot 10^{10}$ had been reached in a vertical, differentially heated, rectangular channel. The channel height in the simulations is successively increased from the original $0.38\,m$ to at least $15\,m$ to achieve CFD results for large Rayleigh-number

configurations. The heat transfer is calculated along each heated wall height from simulation results to develop heat transfer correlations to describe free convection for $\mathrm{Ra} > 10^{12}$, as currently no experimental data is available to directly validate the simulations.

REFERENCE EXPERIMENT

Giel & Schmidt used a water-filled vessel with a height $Y = 384\ mm$, a height-to-width ratio of $\theta_{YX} = 10$ and a height-to-depth ratio of $\theta_{YZ} = 5$ as shown in Figure 1. Based on the system configuration, the authors stated that the Rayleigh-number achieved was $\mathrm{Ra} \sim 8 \cdot 10^{10}$, with a Prandtl-number $\mathrm{Pr}(\bar{T}) \sim 3.1$ at averaged temperature $\bar{T}$. The sidewalls were made entirely of copper with a wall thickness of $X_{cp} = 9.5\ mm$. The left copper plate was electrically heated at $T_h = 343.15\ K$, resulting in a temperature profile along the height $T(y)$ with $y \in Y$ on the inside. The opposing wall was kept constantly at $T_c = 318.15\ K$. The configuration was surrounded by $5\ cm$ of insulation on the sides, top and bottom. The temperature measurements were performed with thermocouples and the flow field velocity was measured by Laser Doppler anemometry.

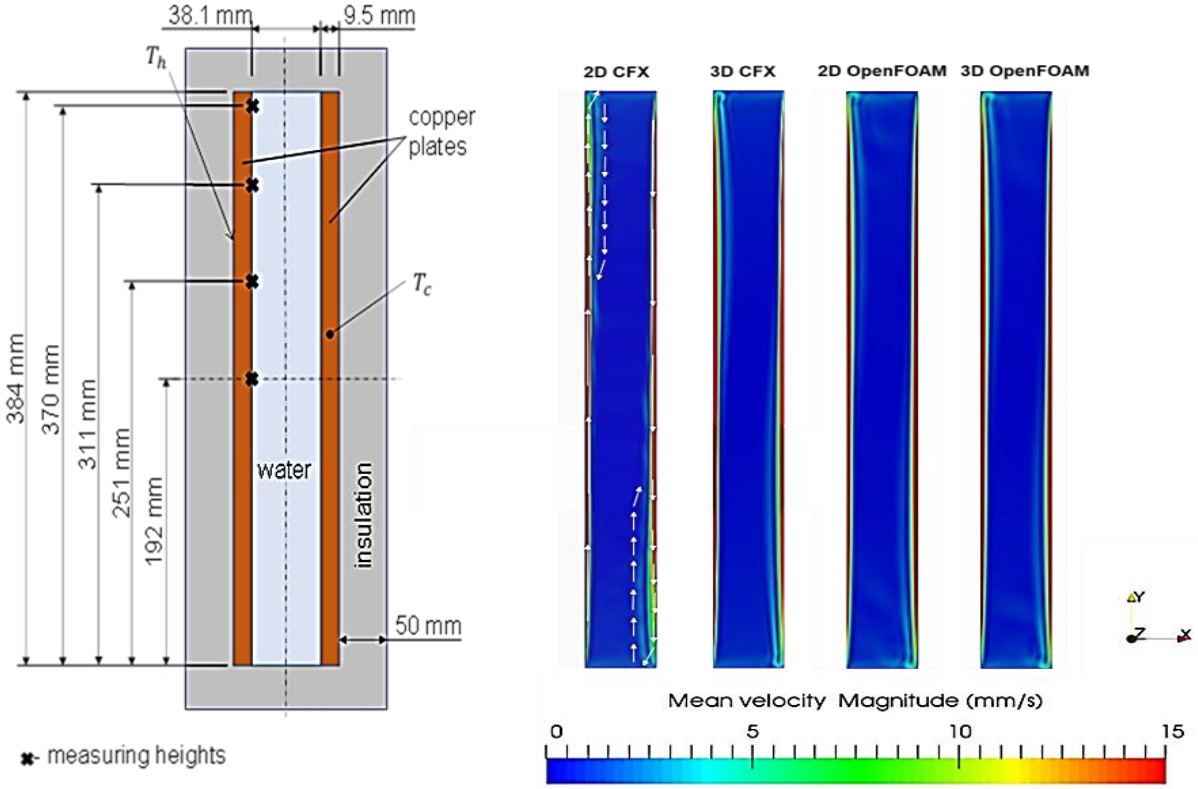

Figure 1: Configuration of the Giel & Schmidt experiment and comparison of the calculated distributions for the mean velocity magnitude

MODELLING

In the following part, the modelling of the reference experiment is described for both, the CFX and the OpenFOAM environment. In general, a dimensionless distance of the wall-adjacent cell centroid is constantly maintained at $y^+ \sim 1$ for the meshes to resolve the boundary layers explicitly. The meshes consist of rectangular hexahedral cells. The geometric parameters are set according to the experimental reference.

SETUP IN CFX

The CFD-Software ASYS CFX 19.2 is used in the work of GRS. The LES WALE (Large Eddy Simulation with Wall-Adapted Local Eddy-viscosity model [4]) is used for turbulent flow. This model is based on the square of the velocity gradient tensor and is more adaptive for wall bounded flows than the traditional Smagorinsky subgrid-scale model [4]. The Automatic near-wall treatment [5] is used, which automatically switches from wall-functions to a low-Re near wall formulation as the mesh is refined. In addition, the buoyancy model is turned on to account for natural convection flow.

The material properties of water with temperature dependency of specific heat capacity, density, conductivity and dynamic viscosity are obtained from the IAPWS Industrial Formulation 1997 for the thermodynamic properties of water and steam.

The simulation domain is composed of a fluid region for the water-filled vessel und two solid regions for the heated sidewall and cold sidewall. The fluid domain and the solid domain are coupled using interface boundary conditions which allow the consideration of the heat transfer between fluid and solid and thus the simulations of the conjugated heat transfer (CHT). The temperature of the outside of the heated wall and cold wall is set to constant as in the experiment. The top wall and bottom wall are set adiabatic. The half vessel with $38\ mm$ depth is calculated in the 3D simulation.

SETUP IN OPENFOAM

For comparison to the previous setup, in the work of PSS a compressible, transient heat transfer solver for buoyancy driven flows *buoyantPimpleFoam* is used in OpenFOAM v2006. For buoyancy generation the Boussinesq-Approximation is chosen to account for density gradients, which solely depends on temperature differences. This leads to an incompressible consideration of the transport equations for mass, momentum and energy. Further the transport equations are solved in terms of a Reynolds-averaged formulation due to the usage of a RANS-based (Reynolds Averaged Navier Stokes) turbulence model. According to this, the transported quantities, generically represented by ϕ, are split into an averaged part Φ and a fluctuating part ϕ' like $\phi = \Phi + \phi'$. The fluctuating part of the quantity is modelled in terms of the eddy viscosity in the momentum equation and the thermal eddy diffusivity in the energy equation. The turbulence model used for the simulations is the k-ω-SST-SAS by Menter & Egorov [6; 7]. It is a two-equation model using the turbulent kinetic energy k and the specific eddy dissipation rate ω with additional blending between the near wall region and the free flow region based on the well-known k-ω-SST-model [8]. The SAS-model (Scale Adaptive Simulation) is an enhanced approach that applies an additional strategy to account for varying turbulent length scale in the flow via instantaneous flow conditions. The OpenFOAM implementation can be found in [9].

All thermophysical properties are kept constant during the simulations. Preliminary simulations using temperature-dependent polynomials for thermophysical properties gave less accurate results than the application of the Boussinesq-Approximation, which has consequently been retained. The individual quantities are set according to the average system temperature.

For the initial mesh $2 \cdot 10^7$ cells are considered in a full 3D mesh to compare with the experimental results. Later, a 2D mesh is considered and used for the scaled simulations. For any wall the *no slip condition* is applied. The heated wall temperature is calculated via the *externalWallHeatFluxTemperature* wall function since a temperature gradient along the wall height is observed in the experimental data. The colder wall temperature is set to constant, while other walls are set adiabatic.

RESULTS

In this section, the results of the simulations with the two different approaches are reported and evaluated. First, the error resulting from the 3D to 2D transformation is discussed. This transformation is needed because of the increasing computational effort to solve the transient flow field in 3D until a quasi-steady solution is reached. After this, the initial geometry is scaled up to a total vertical wall height of $15\ m$ on a 2D mesh, Finally, the simulation results for the heat transfer are determined from the calculations and compared to different correlations from literature.

In the Figure 1 (right), the calculated distributions for the mean velocity magnitude of 2D- and 3D-simulations with CFX and OpenFOAM are shown. The four profiles all look very similar. The moving flow layer is located in the vicinity of the heated and cold walls. The velocity inside the vessel is very small. The recirculation zone is located at the upper edge of the heated wall and the lower edge of the cold wall.

Figure 2 shows the calculated and the measured mean velocities in Y direction for the specified measurement positions ($Y = 251$ mm and $Y = 370\ mm$, defined in Figure 1) and the calculated and the measured temperature profiles for the same measurement position are shown. The differences in the 2D and 3D CFX and OpenFOAM simulation results are small. These are in good agreement with experimental data, while the CFX results fit slightly better.

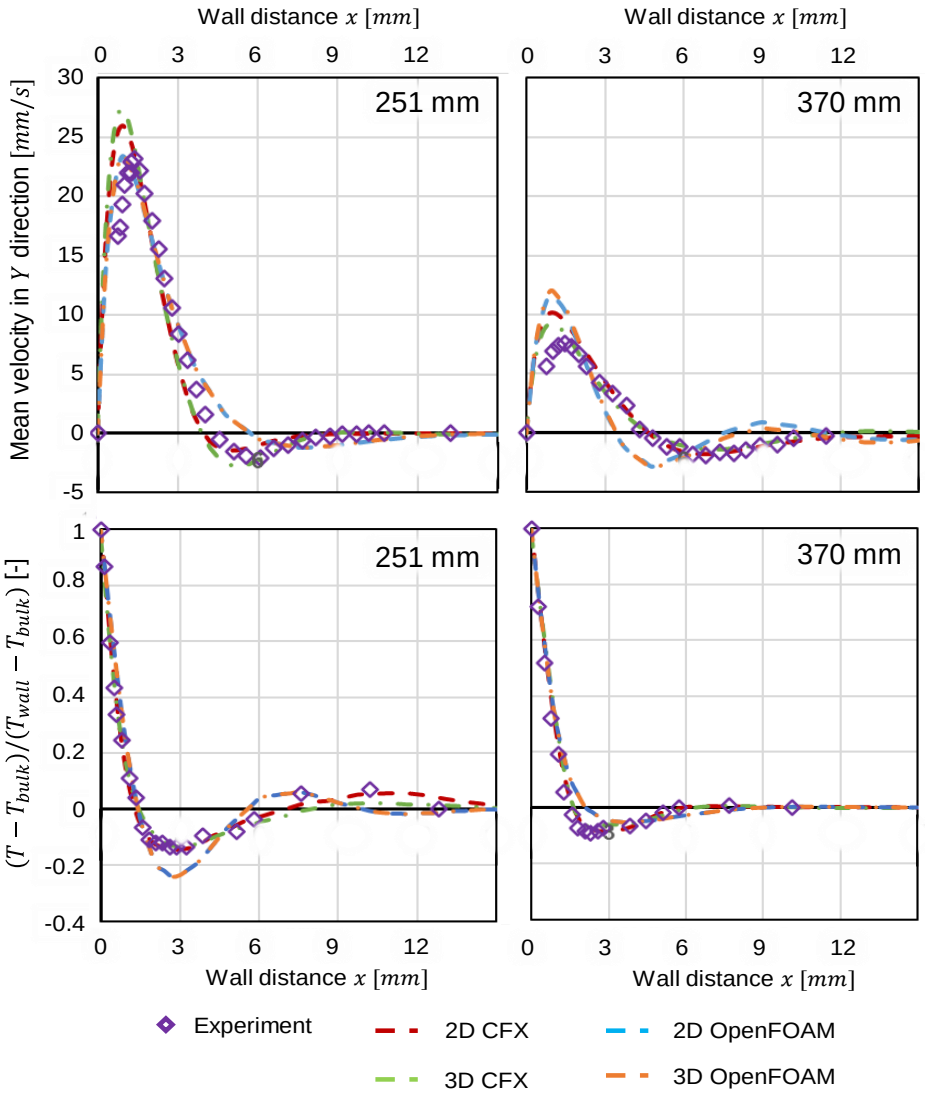

Figure 2: Comparison of the measured and calculated mean velocities in Y direction and the dimensionless temperatures

In the work of PSS, five upscaled geometries with heights of $1m$, $2.5m$, $5m$, $10m$ and $15m$ are simulated with OpenFOAM. The calculated results for the mean Nusselt- and Rayleigh-numbers are presented in Figure 3 (Nu_sim OpenFOAM). A new correlation (Nu_OpenFOAM) is derived from these results, by averaging the locally calculated heat transfer coefficients along each wall height. The progression of the results for each wall height fits to a potential function similar to the definitions of e. g. Fujii & Imura [10] and Nansteel & Greif [11] but with deviating constants. The resulting *coefficient of determination* is $R^2 = 0.9992$ and the relative error of each derived constant is about $0.8\ \%$ regarding the simulation

results. In the work of GRS, four upscaled geometries with heights $1\,m$, $3\,m$, $5\,m$ and $15\,m$ with the same wall temperature as in the Giel & Schmidt experiment are simulated with CFX. Another five simulations with the validated wall temperatures for ($\mathrm{Pr} = 2.3, 4.58$ and 6.54) are performed. From these simulation results, a new correlation is derived similar to the formulation of McAdams [12] by fitting the constants to the simulation results and accounting for changes in Pr. The statistical coherence to the simulation results is defined by $R^2 = 0.99$ and a relative deviation of $4\,\%$ to $-5\,\%$ in the progression. The calculated results for the Nusselt- and Rayleigh-numbers (Nu_sim CFX) and the new correlation (Nu_CFX) are shown in Figure 3 as well. The calculated Nusselt-numbers represent the integral heat transfer along the heated wall. The available empirical correlations for integral Nusselt-numbers from Churchill & Chu [13], Fujii & Imura [10], McAdams [12] and Nansteel & Greif [11] are schown in the Figure 3 for comparisson. The range of the empirical correlations is only claimed to be valid for Rayleigh-numbers of $\leq 10^{12}$ reliably. In this region, differences between the empirical und the calculated Nu-correlations are small. The CFX results match best with [12] with a relative deviation between $8\,\%$ for the initial wall height and $14\,\%$ for the $1\,m$ wall height. The OpenFOAM results on the other hand match best with [10] without deviation for the initial geometry and incresing deviations while aligning to the CFX correlation until $\mathrm{Ra} \sim 10^{13}$ and to [12] along the further progression. As the Rayleigh-number increases, the deviation between the correlation of [12]and the derived correlation from CFX simulations increases. The largest daviations can be observed for [10] and [11] in comparisson to the simulation results at $\mathrm{Ra} > 10^{12}$ and can therefore be excluded for the heat transfer predictions at larger Rayleigh-numbers.

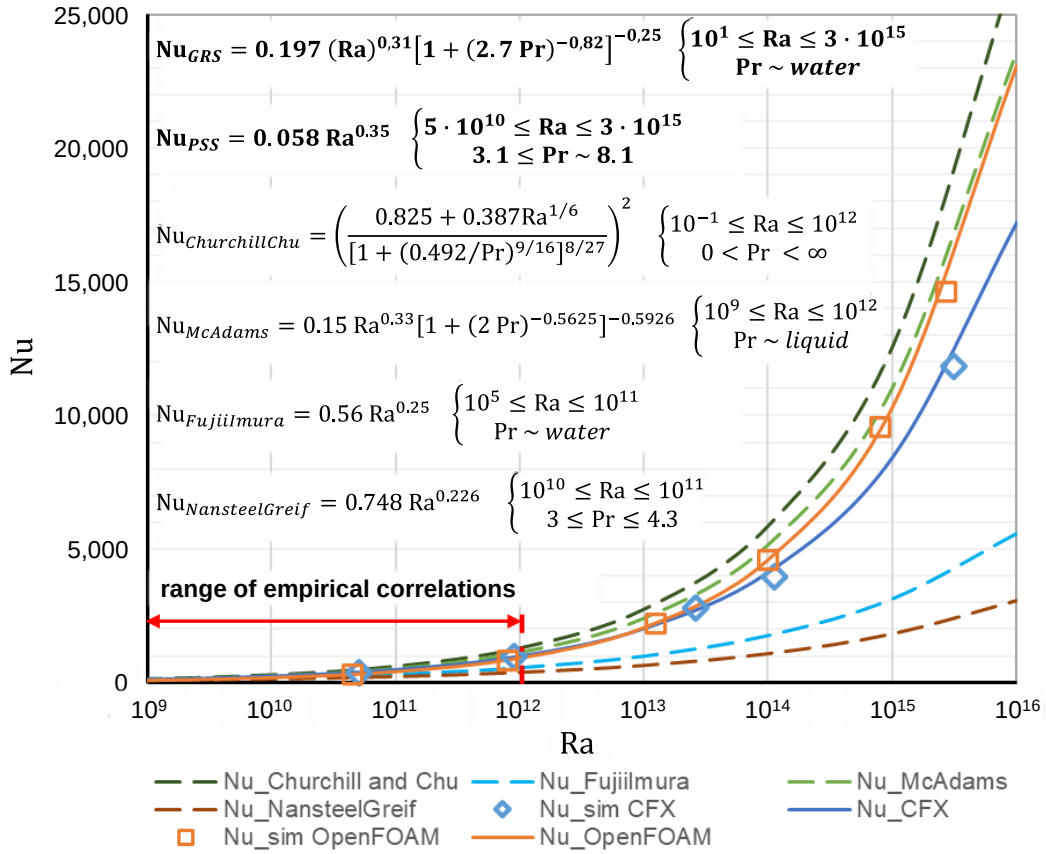

Figure 3: Comparison of the empirical and calculated Nu-correlations

The simulation results of CFX and OpenFOAM lie all relatively close to each other in the range from $\mathrm{Ra} = 10^{10}$ to $\mathrm{Ra} = 10^{14}$. In the region with $\mathrm{Ra} > 10^{14}$, where very strong turbulence occurs, the simulation results of CFX differ from the OpenFOAM results due to the different turbulence modelling. The LES with an additional buoyancy model is more reliable than the SAS, also considering the variable thermophysical properties applied in the CFX simulations. However, a degree of uncertainties remains due to mostly 2D considerations in the simulations and missing experimental data for large wall heights for the final validation.

CONCLUSION

In this work, the 2D- und 3D- simulations of ANSYS CFX and OpenFOAM are validated against the experiment of Giel & Schmidt. The calculated temperature and velocity in the channel at different heights are compared to the experimental data. Good agreement between simulation and experiment is observed. The height of the simulated channel is gradually increased from $0.38\,m$ to $15\,m$, while the aspect ratio remained constant at $10{:}\,1$. Series of simulations are performed with both CFD tools. In the case with $15\,m$ wall height, the Rayleigh-number reached is $3 \cdot 10^{15}$. In this way, correlations for the average Nusselt-number are determined from the results of simulations which are then compared to empirical correlations from literature.

ACKNOWLEDGEMENT

Supported by:

Federal Ministry
for the Environment, Nature Conservation,
Nuclear Safety and Consumer Protection

based on a decision of
the German Bundestag

This work was funded by the German Federal Ministry for the Environment, Nature Conservation, Nuclear Safety and Consumer Protection (BMUV) under grant numbers RS1585A and 1501607B based on a decision of the German Bundestag. Project partners of the consortium are Gesellschaft für Anlagen- und Reaktorsicherheit (GRS) gGmbH, Institute of Nuclear Technology and Energy Systems (IKE) of the University of Stuttgart and Plant Simulation and Safety Group (PSS) of Ruhr-Universität Bochum. The results were obtained using OpenFOAM v2006 of OpenCFD Ltd. © and CFX 19.2 of ANSYS Inc.

REFERENCES

1. N. Jiang, M. Peng, W. Wei and T. Cong, "Strategy Evaluation for Cavity Flooding during an ESBO Initiated Severe Accident," *Science and Technology of Nuclear Installations*, 2018, pp. 1–15 (2018).
2. B.R. Sehgal, "*Nuclear Safety in Light Water Reactors - Severe Accident Phenomenology*," 1 - Elsevier Academic Press (2012).
3. Giel, P. W.; Schmidt, F. W., "An Experimental Study of High Rayleigh Number Natural Convection in an Enclosure," *Proceedings of the 8th International Heat Transfer Conference Digital Library*, 0-89116-559-2 (1986).
4. J. Smagorinsky, "General circulation experiments with the primitive equations: I. The basic experiment," *Monthly Weather Review* - American Meteorological Society, 3, pp. 99–164 (1963).
5. ANSYS, Inc., "*ANSYS CFX-Solver Modelling Guide - Release 19.2*," (2019).
6. F.R. Menter and Y. Egorov, "The Scale-Adaptive Simulation Method for Unsteady Turbulent Flow Predictions. - Part 1: Theory and Model Description," *Flow Turbulence Combustion* - Springer Science+Business Media (85), pp. 113–138 (2010).
7. F.R. Menter, "Best practice: scale-resolving simulations in ANSYS CFD," *ANSYS Germany GmbH* (2012).
8. Menter, F. R.; Esch, T., "Elements of industrial heat transfer predictions," *Proceedings of the 16th Brazilian Congress of Mechanical Engineering (COBEM)*, Vol.20, 11 (2001).
9. "kOmegaSSTSAS - Turbulence Model - OpenFOAM v2012 Extended Code Guide," https://www.openfoam.com/documentation/guides/latest/api/classFoam_1_1RASModels_1_1kOmegaSSTSAS.html (2020).
10. T. Fujii and H. Imura, "Natural-convection heat transfer from a plate with arbitrary inclination," *International Journal of Heat and Mass Transfer*, 15 (4), pp. 755–764 (1972).
11. M.W. Nansteel and R. Greif, "Natural Convection in Undivided and Partially Divided Rectangular Enclosures," *Journal of Heat Transfer* - American Society of Mechanical Engineers Digital Collection, 4, pp. 623–629 (1981).
12. W.H. McAdams, "*Heat Transmission*," - McGraw-Hill Book Company, New York, USA (1954).
13. S.W. Churchill and H.H. S. Chu, "Correlating equations for laminar and turbulent free convection from a vertical plate," *International Journal of Heat and Mass Transfer*, 18, pp. 1323–1329 (1975).